

A New Compact Circular Shape Fractal Antenna for Broadband Wireless Communication Applications

Aliakbar Dastranj*, Fatemeh Ranjbar, and Mosayeb Bornapour

Abstract—A new compact broadband circular fractal antenna is presented to simultaneously cover the operations in S-, C-, X-, and Ku-bands. Fractal geometry of the radiator including an iterative circular patch with a square slot, a modified feed-line with step technique, and slot-loaded semi-circular ground plane is used to achieve a broad impedance bandwidth more than 151% from 3 to 21.5 GHz ($|S_{11}| < -10$ dB). The simulation results are verified by experimental measurements. Measured data are in good agreement with the simulated results. The frequency- and time-domain characteristics of the antenna including impedance matching, far-field patterns, gain, group delay, and fidelity factor are presented and discussed. The proposed broadband antenna features small size of $38 \times 36 \times 1.4$ mm³ and nearly omnidirectional radiation patterns that make it excellent candidate for integration in broadband wireless communication systems.

1. INTRODUCTION

Nowadays, broadband wireless communication technology has received widespread concentration due to its great capacity, high data rates, low operating power level, and low complexity. The modern wideband wireless communication systems need miniaturized and wideband antennas with high radiation efficiency. These mechanical and electromagnetic specifications have required the development of novel antenna structures.

Printed fractal antennas have attracted much attention in wireless communication because of their low profile, small cost, and ease of manufacture [1]. These antennas have shown the possibility to miniaturize antenna systems and improve input impedance matching. Also, a fractal antenna can be designed to operate over a wide range of frequencies using the self-similarity properties associated with fractal geometry structures. Planar fractal antennas can be used in variety of wideband applications, especially where space is limited. The geometry of fractal antenna was defined by Mandelbort in 1975 [2]. A fractal is a self-similar geometric shape of the whole structure which can be subdivided into parts; each of the parts is a reduced size copy of the whole geometry of the antenna [3]. Fractal geometry has some advantages over simple planar radiator such as: at arbitrarily minute scale it has an excellent structure, and it can be easily described in traditional Euclidean geometry and has simple and recursive structure. Also, fractal geometry improves input resistance and enhances electrical area of antenna [4]. Thus, to miniaturize the antenna size with high radiation efficiency, fractal antennas are most suitable [5].

In the past few years, to satisfy the wideband communication systems requirements, several researches on fractal antennas have been reported [6–10]. In [6], a fractal monopole antenna with a volume of $24 \times 24 \times 1$ mm³ can cover a bandwidth of 2.1–11.52 GHz. In [7], a co-planar waveguide (CPW)-fed octagonal Sierpinski fractal antenna can cover a bandwidth of 3.73–20 GHz. A multiband Koch-like sided fractal bow-tie dipole antenna was reported in [8]. The fractal printed bow-tie antenna in [9] can

Received 10 March 2019, Accepted 22 May 2019, Scheduled 30 May 2019

* Corresponding author: Aliakbar Dastranj (dastranj@yu.ac.ir).

The authors are with the Electrical Engineering Department, Faculty of Engineering, Yasouj University, Yasouj 75918-74831, Iran.

cover a bandwidth from 1.64 to 1.94 GHz. In [10], an antenna with notch-band characteristics which uses Koch fractal for ultra-wideband (UWB) applications was proposed. Different fractal antennas for wideband application were reported in [11–13]. In [11], a circular-hexagonal fractal antenna was investigated for many wireless communications systems such as ISM, Wi-Fi, GPS, Bluetooth, WLAN, and UWB. It was made of iterations of a hexagonal slot inside a circular metallic patch with a transmission line. A partial ground plane and asymmetrical patch toward the substrate were used for designing the antenna to achieve a wide bandwidth. In [12], a hexagon-shaped fractal antenna with a triangular slot and a total size of $20 \times 33.4 \times 1.57 \text{ mm}^3$ for wideband application was presented. In [13], a printed star-triangular fractal microstrip-fed monopole antenna with semielliptical ground plane was presented for wideband applications. A miniaturized UWB antenna based on Sierpinski square slots was reported in [14]. It had a compact dimension of only $28 \times 28 \text{ mm}^2$ and a fractional bandwidth about 127.3% (3.41–15.37 GHz). A printed Koch snowflake antenna with an operating frequency range of 3.4–16.4 GHz for UWB radio frequency identification applications was presented in [15]. Also some fractal antennas were designed for multiband operation [16–19].

The objective of this paper is to design a miniaturized broadband antenna with a simple structure and satisfactory radiation characteristics, using fractal elements. Another important issue is to keep the antenna inexpensive and easy to manufacture. To accomplish these goals, a circular fractal antenna with 6 iterations is proposed. To achieve broadband impedance bandwidth with suitable radiation pattern, we use a new fractal circular radiator fed by a stepped microstrip feed-line along with a square shaped slot in semi-circular ground plane. In order to match the antenna to the 50Ω SMA connector, a multi-section microstrip line of different widths is designed. The novelty of the proposed design lies in its simple fractal structure, compact size, and broadband operation along with high radiation efficiency. The simulation results obtained from HFSS simulator package are verified by experimental measurements. The proposed printed fractal antenna with a compact size of $38 \times 36 \times 1.4 \text{ mm}^3$ can cover S-, C-, X-, and Ku-bands from 3 to 21.5 GHz (151% impedance bandwidth defined by -10-dB reflection coefficient). Measured results show that the designed antenna features desirable frequency-domain characteristics such as nearly omnidirectional radiation patterns, high radiation efficiency, and reasonable gain. Furthermore, to analyze the proposed antenna in time domain, group delay and fidelity factor are investigated. The antenna has advantages of compact size, low manufacturing cost, easy fabrication, low profile, wide operating bandwidth, and small ground plane suitable for integration with compact broadband communication systems.

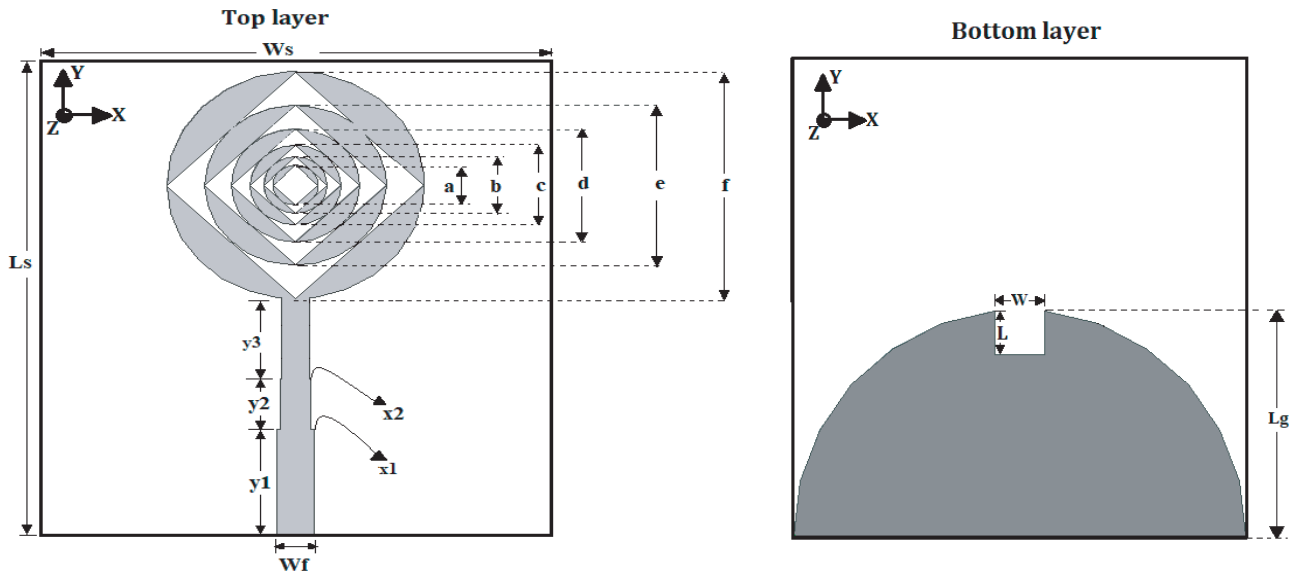


Figure 1. Antenna geometry and design parameters.

2. FRACTAL ANTENNA DESIGN AND DEVELOPMENT STAGES

The geometry of the proposed super-wideband (SWB) antenna is shown in Figure 1. It is etched on a 1.4 mm thick FR-4 epoxy ($\epsilon_r = 4.4$, $\tan \delta = 0.02$) substrate. The copper cladding's thickness and the total size of the antenna are $35 \mu\text{m}$ and $36 \times 34 \times 1.4 \text{mm}^3$, respectively. The antenna consists of a semi-circular ground plane and fractal circular radiator that is fed by a stepped microstrip feed-line. The microstrip feed-line is stepped to achieve smooth transmission between the models and wider bandwidth. Also, to obtain better impedance matching, the conventional rectangular ground plane is replaced by semi-circular ground plane. It is further loaded with a rectangular slot at the feeding location to improve the impedance bandwidth. The radiator is made of a 6-iteration fractal structure.

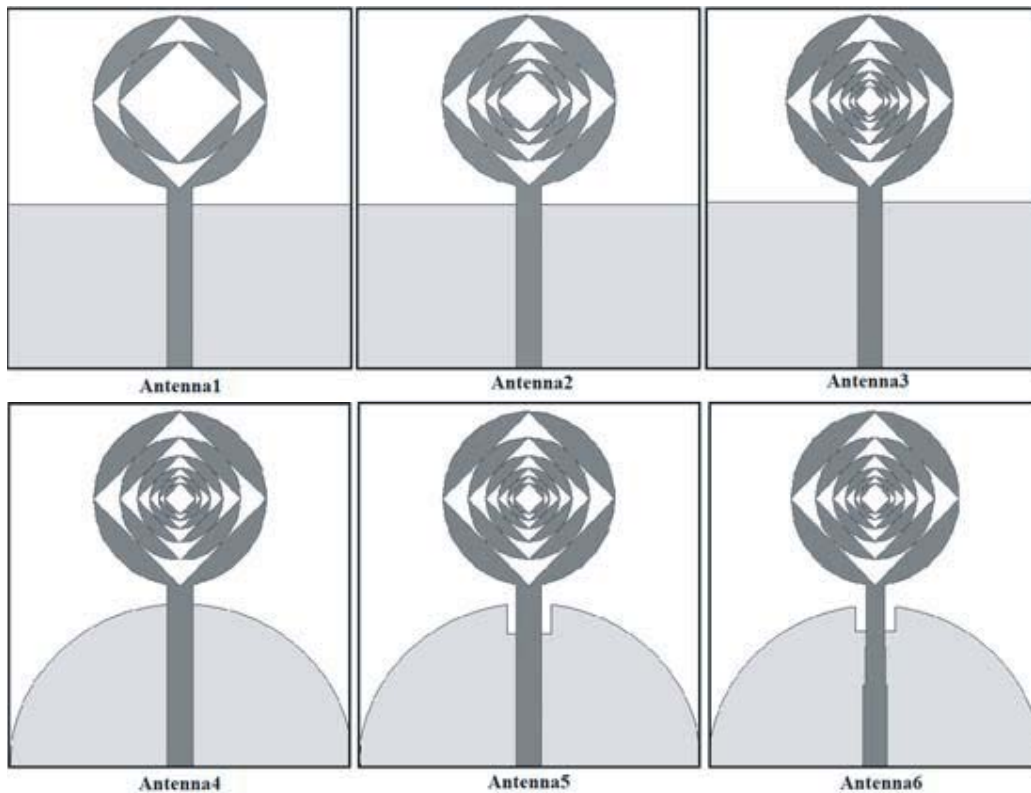


Figure 2. Stages of the antenna design.

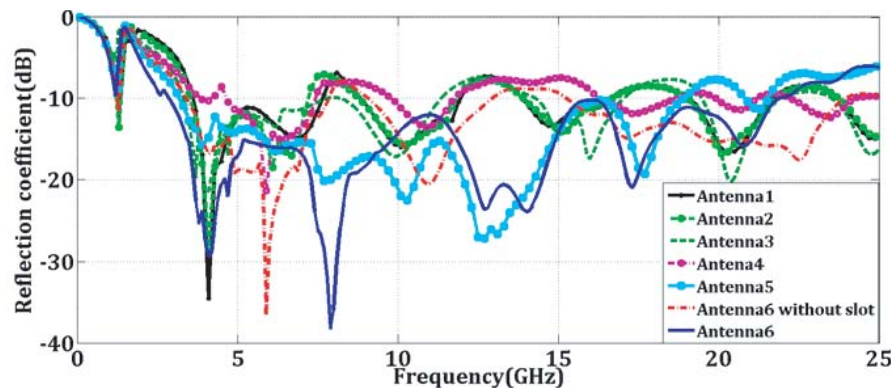


Figure 3. Simulated reflection coefficient curves of the antennas corresponding to Figure 2.

Each iteration of the fractal structure is composed of a circle from which an inscribed square has been subtracted. The relationship between each iteration fractal structure and previous iterations according to the parameters in Figure 1 is as follows:

$$f = 18m, \quad e = \frac{f}{1.4}, \quad d = \frac{e}{1.4}, \quad c = \frac{d}{1.4}, \quad b = \frac{c}{1.4}, \quad a = \frac{b}{1.4} \quad (1)$$

In Figures 1, a, b, c, d, e, and f are radii of the iterative circular patches. The development stages of the proposed antenna are illustrated in Figure 2, and the corresponding simulated reflection coefficient curves are plotted in Figure 3. The first antenna consists of a common microstrip feed-line with $50\ \Omega$ impedance, rectangular ground plane, and radiator with 2 iterations fractal. In the second antenna,

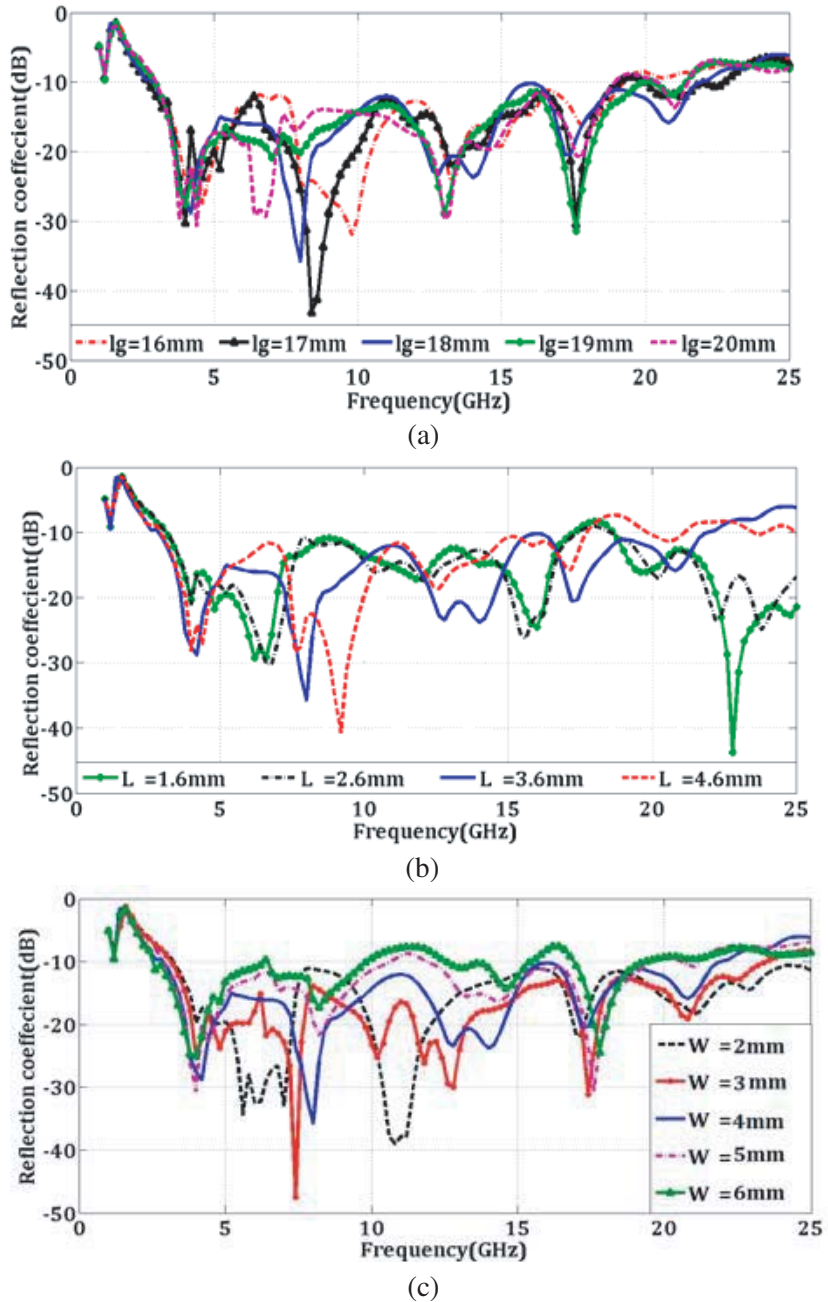


Figure 4. Influence of lg , L and W on the impedance bandwidth of the antenna. (a) lg , (b) L , (c) W .

two fractal iterations are added to radiator of the first antenna, and also in the 3rd antenna, two fractal iterations are added to previous antenna. At the 4th antenna, rectangular ground plane is replaced by semicircular ground plane. At the next step, a rectangular slot with a dimension of $4 \times 3.6 \text{ mm}^2$ is applied to the ground plane. Finally, at the 6th step, we apply step technique to the feed-line. This technique increases bandwidth, both at the beginning and end of the frequency band. Antenna 6 is the final proposed antenna. The geometrical parameters of the proposed antenna are as follows: $Ws = 36 \text{ mm}$, $Ls = 38 \text{ mm}$, $Wf = 2.7 \text{ mm}$, $y1 = 8.5 \text{ mm}$, $y2 = 4 \text{ mm}$, $y3 = 6.5 \text{ mm}$, $x1 = 0.25 \text{ mm}$, $x2 = 0.1 \text{ mm}$, $W = 4 \text{ mm}$, $L = 3.6 \text{ mm}$, and $lg = 18 \text{ mm}$.

Numerical parametric analysis via Ansoft HFSS was performed to understand the influence of the antenna physical dimensions on the impedance bandwidth. The reflection coefficient curves for three important parameters are shown in Figure 4. This figure shows selecting the optimal values of $lg = 18 \text{ mm}$, $W = 4 \text{ mm}$, and $L = 3.6 \text{ mm}$ leads to the widest bandwidth. As depicted in Figure 4(a), by increasing lg from 16 to 18 mm, the upper frequency of the bandwidth is shifted from 20 to 22.2 GHz. However, by further increasing lg to 20 mm, the higher band edge frequency of the bandwidth is shifted down from 22.2 to 19 GHz, and consequently the impedance bandwidth of the antenna decreases. It is seen in Figure 4(b) that by increasing rectangular slot length L to 3.6 mm, the upper frequency of the bandwidth increases from 18 to 22.2 GHz, resulting in the improvement of the impedance bandwidth over higher frequencies. This figure shows that for larger values of L , the antenna reflection coefficient deteriorates. The influence of variation of rectangular slot width W is presented in Figure 4(c). Results of this figure show that the optimum value of W for maximum impedance bandwidth is 4 mm.

3. EXPERIMENTAL VERIFICATION AND DISCUSSION

In order to validate the numerical results obtained by Ansoft HFSS, the designed fractal antenna was constructed and tested. Figure 5 shows photographs of the fabricated prototype. In the following, the experimental outcomes are given, discussed, and compared with the numerical results.

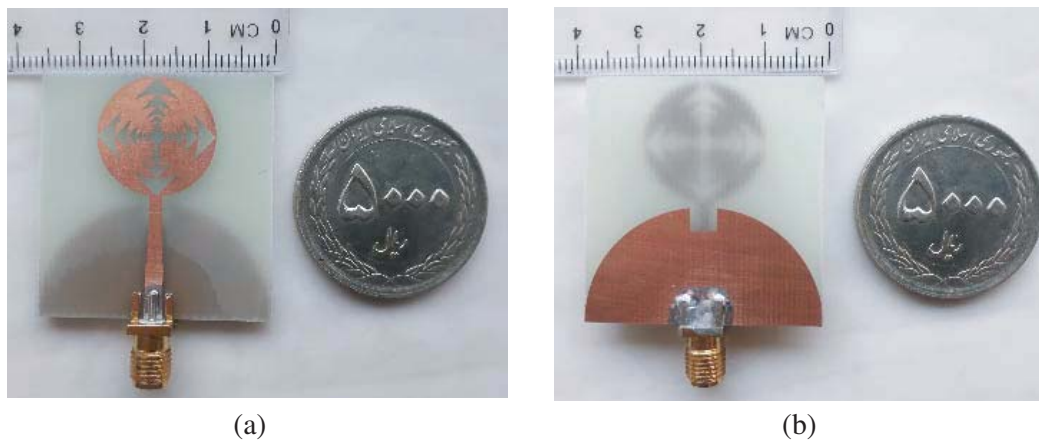


Figure 5. Top and bottom views of the fabricated prototype ((a) top, (b) bottom).

3.1. Frequency-Domain Results

Figure 6 presents the comparison of experimental and numerical reflection coefficient curves of the proposed antenna. Measured and simulated results show that the proposed fractal antenna can cover a SWB frequency range, from 3 to 21.5 GHz (151% impedance bandwidth). The discrepancies between the experimental result and numerical data are due to measurement errors and test equipment. However, to determine the overall bandwidth of the antenna, other radiation characteristics such as radiation patterns and gain must also be carefully examined over the entire frequency band. The co- and cross-polar far-field radiation patterns of the antenna were measured at different frequencies. For brevity,

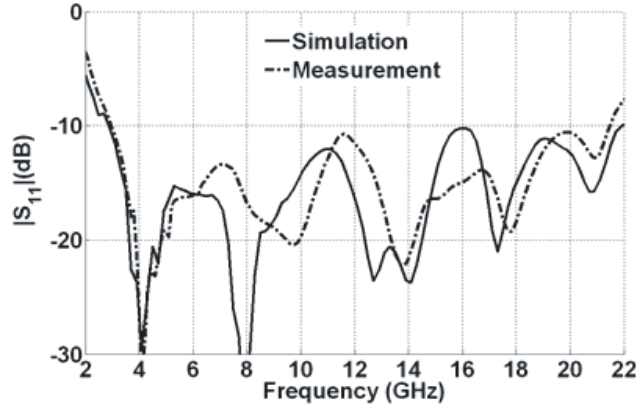
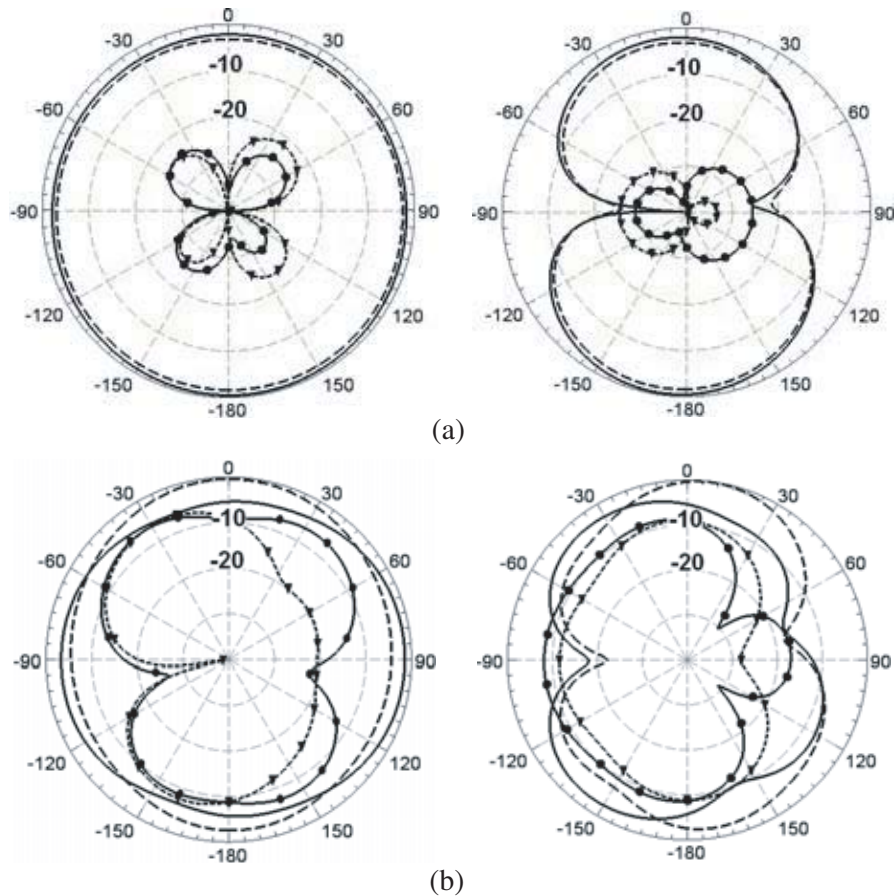


Figure 6. Numerical and experimental reflection coefficient curves of the antenna.

the numerical and experimental H (x - z) and E (y - z) plane patterns at only 3, 8, 13, 17, and 21 GHz are compared in Figure 7. A good concordance between the numerical and experimental outcomes is observed. As illustrated in this figure, the antenna features nearly omnidirectional patterns specifically in the x - z plane. The increase in cross-polarization level is due to the excitation of hybrid current distribution on the antenna radiator at high frequencies. Figure 8 plots the simulated and measured gain curves of the proposed antenna versus frequency. The measured gain has an average value of 2.88 dB, and the maximum value of the measured antenna gain is 5 dB which occurs at 15 GHz. It should be noted that the antenna gain is moderate over the working band respecting the compact



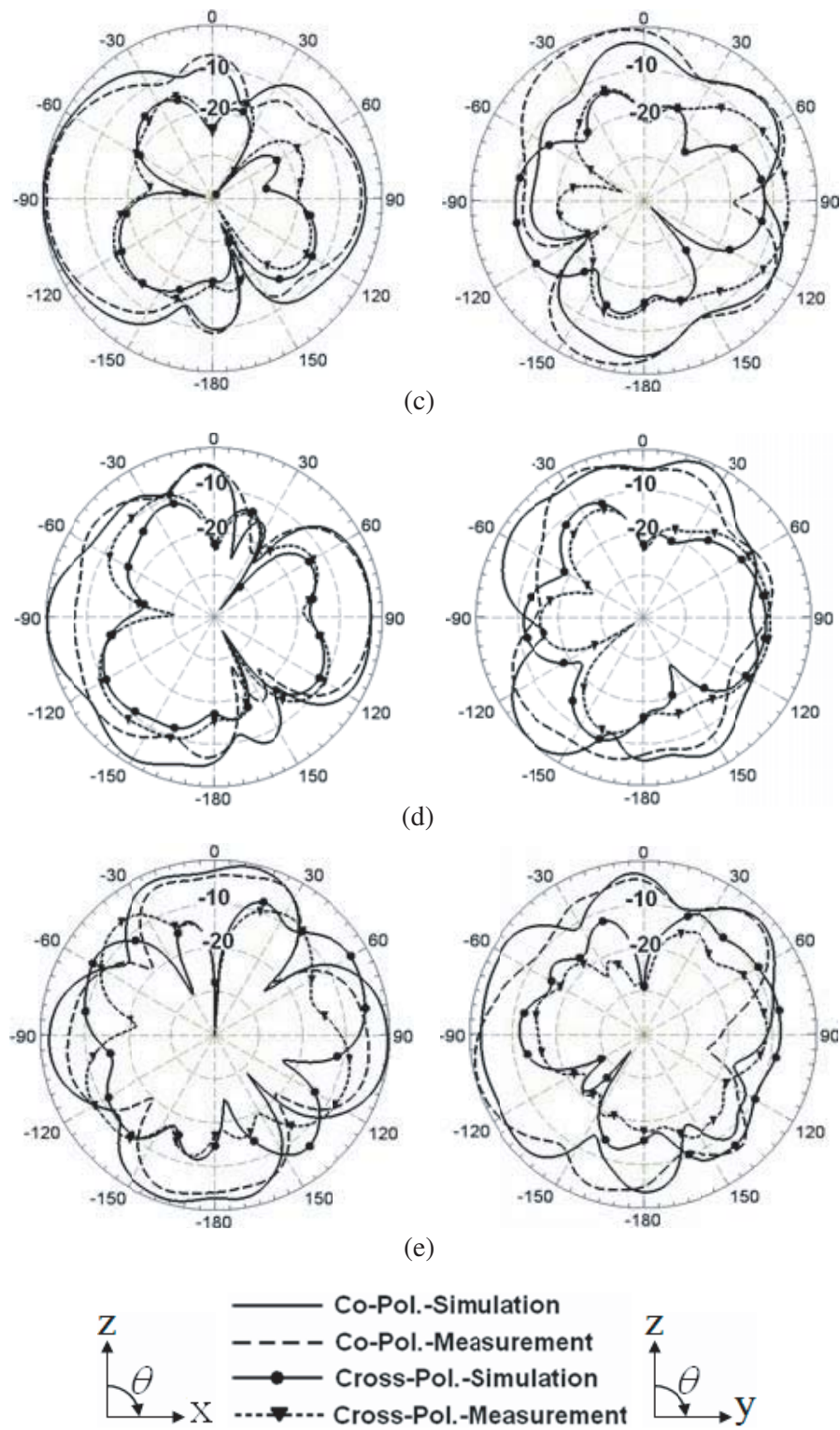


Figure 7. Experimental and numerical far-field E (Y - Z)-and H (X - Z)-plane patterns of the antenna (left: X - Z plane, right: Y - Z plane) at (a) 3 GHz, (b) 8 GHz, (c) 13 GHz, (d) 17 GHz, and (e) 21 GHz.

size and omnidirectional behavior of the antenna. In order to measure the gain of the fabricated antenna, the gain-transfer (gain-comparison) method was used [20]. The procedure requires two sets of measurements. In one set, using the test antenna as the receiving antenna, and the received power (PT) into a matched load was recorded. In the other set, the test antenna was replaced by the standard gain antenna, and the received power (PS) into a matched load was recorded. In both sets, the geometrical arrangement was maintained intact (other than replacing the receiving antennas), and the input power was maintained the same. The gain of the antenna under test can be found by the following equation:

$$(GT) \text{ dB} = (GS) \text{ dB} + 10 \log(PT/PS) \quad (2)$$

where $(GT) \text{ dB}$ and $(GS) \text{ dB}$ are the gains (in dB) of the test and standard gain antennas [20].

3.2. Time-Domain Results

In order to analyze the time-domain performance of the designed SWB fractal antenna, group delay and fidelity factor parameters are investigated. To provide desirable time-domain behavior, constant group delay is required over the entire working band. Figure 9 presents the measured and simulated group delay curves of the proposed fractal antenna for face-to-face case. To investigate the group delay, the distance between the receiving and transmitting antennas was selected as 500 mm. As shown in Figure 9, the peak-to-peak variation of the measured group delay is limited to less than 2 ns over the whole working band. The results indicate that the proposed antenna has an acceptable time domain response. Although they were not shown, similar results for side-by-side configuration were obtained.

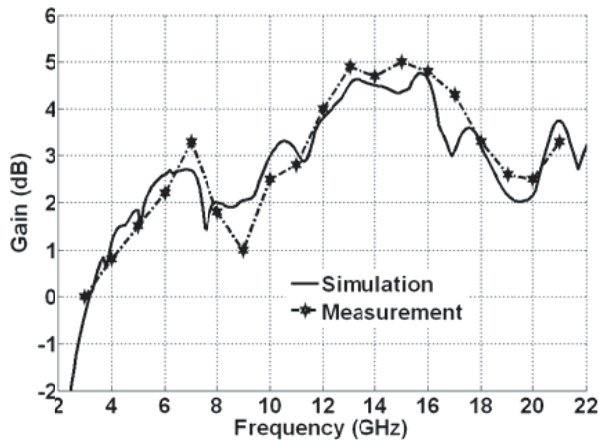


Figure 8. Numerical and experimental gain curves of the antenna versus frequency.

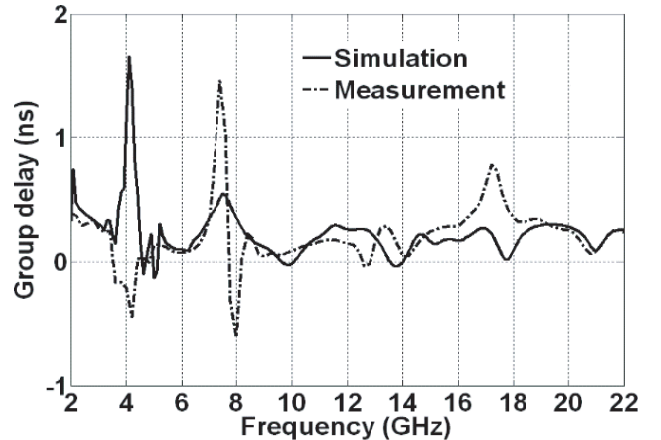


Figure 9. Experimental and numerical group delay results of the antenna versus frequency.

The fidelity factor is generally preferred as a time domain performance parameter. In the last step of this work, fidelity factor is calculated by using CST Microwave Studio. By utilizing the approach presented in [21], the input pulse is delivered to the antenna, and the electric component in the far-field region is received via four virtual probes. The distance between the transmitting antenna and probes maintains at 500 mm. The fidelity factor is calculated in both E - and H -planes. In each plane, four probes are located with the angle equal to 0° , 30° , 60° , and 90° , respectively. The calculated fidelity factor for both planes is presented in Table 1. As can be observed, the fidelity factor in both planes is more than 0.79, making the antenna suitable for most practical SWB applications. The experimental results in frequency as well as time domain indicate that the antenna is an excellent option for SWB wireless communication applications.

Temperature humidity test chamber is able to simulate a wide range of temperature and humidity environments. It was used in testing fabricated antenna for its tolerances of heat, cold, dry, and humidity. It is found that operating temperatures range from -40°C to $+550^\circ\text{C}$, and humidity range is from 20% to 90% RH. These results show that the antenna can perform in environments with a wide range of operating temperatures and humidity.

Table 1. Calculate fidelity factor of the antenna.

Angle (degrees)	Fidelity factor	
	<i>E</i> -plane	<i>H</i> -plane
0	0.92	0.93
30	0.87	0.89
60	0.84	0.86
90	0.79	0.80

4. CONCLUSION

This paper presents a compact SWB antenna with fractal structure for wireless communication systems. It can cover frequency range from 3 to 21.5 GHz. The antenna consists of a printed fractal radiator and a semi-circular ground plane with a rectangular slot. The fractal patch is fed by a stepped microstrip feed-line. Using fractal structure in patch causes miniaturized dimension of antenna and wider bandwidth, and does not need complicated impedance transformer sections. The antenna with an overall size of $38 \times 36 \times 1.4 \text{ mm}^3$ is a good option for use in broadband applications. The frequency and time-domain characteristics of the antenna were analyzed with numerical simulation and experimental measurement.

REFERENCES

- Li, D. and J.-F. Mao, "Sierpinski-like sided multifractal dipole antenna," *Progress In Electromagnetics Research*, Vol. 130, 207–224, 2012.
- Mandelbrot, *The Fractal Geometry of Nature*, W. H. Freeman, New York, 1983.
- Kharat, K., S. Dhoot, and J. Vajpai, "Design of compact multiband fractal antenna for WLAN and WiMAX Applications," *IEEE International Conference on Pervasive Computing (ICPC)*, 2015.
- Werner, D. H. and S. Ganguly, "An overview of Fractal antenna engineering research," *IEEE Antennas and Propagation Magazine*, Vol. 45, 38–57, 2003.
- Gianvittorio, J. and Y. Rahmat-Samii, "Fractal element antennas: A compilation of configurations with novel characteristics," *IEEE Antennas and Propagation Society International Symposium*, Salt Lake City, UT, USA, July 16–21, 2000.
- Moghadasi, M. N., R. A. Sadeghzadeh, T. Aribi, T. Sedghi, and B. S. Virdee, "UWB monopole microstrip antenna using fractal tree unit-cells," *Microwave and Optical Technology Letters*, Vol. 54, No. 10, 2366–2370, 2012.
- Singhal, S., P. Singh, and A. K. Singh, "Asymmetrically CPW-FED octagonal Sierpinski UWB fractal antenna," *Microwave and Optical Technology Letter*, Vol. 58, No. 7, July 2016.
- Li, D. and J.-F. Mao, "A Koch-like sided fractal bow-tie dipole antenna," *IEEE Trans. Antennas Propag.*, Vol. 60, No. 5, 2242–2251, 2012.
- Zhong, Y.-W., G.-M. Yang, and L.-R. Zhong, "Gain enhancement of bow-tie antenna using fractal wideband artificial magnetic conductor ground," *Electron. Lett.*, Vol. 51, No. 4, 315–317, 2015.
- Kumar Terlapu, S., Ch. Jaya, and G. S. Raju, "On the notch band characteristics of Koch fractal antenna for UWB applications," *International Journal of Control Theory and Applications*, Vol. 10, No. 6, 0974–5572, 2017.
- Dorostkar, M. A., M. T. Islam, and R. Azim, "Design of a novel super wide band circular-hexagonal fractal antenna," *Progress In Electromagnetics Research*, Vol. 139, 229–245, 2013.
- Shahu, B. L., S. Pal, and N. Chattoraj, "Design of super wideband hexagonal-shaped fractal antenna with triangular slot," *Microwave and Optical Technology Letters*, Vol. 57, No. 7, 1659–1662, July 2015.

13. Waladi, V., N. Mohammadi, Y. Zehforoosh, A. Habashi, and J. Nourinia, "A novel Modified Star-Triangular Fractal (MSTF) monopole antenna for super-wideband applications," *IEEE Antennas and Wireless Propagation Letters*, Vol. 12, 651–654, 2013.
14. Tanweer, A., B. K. Subhash, and C. B. Rajashekhar, "A miniaturized decagonal Sierpinski UWB fractal antenna," *Progress In Electromagnetics Research C*, Vol. 84, 161–174, 2018.
15. Tizyi, H., F. Riouch, A. Tribak, A. Najid, and A. Mediavilla, "CPW and microstrip line-fed compact fractal antenna for UWB-RFID applications," *Progress In Electromagnetics Research C*, Vol. 65, 201–209, 2016.
16. Khan, O. M., Z. U. Islam, I. Rashid, F. A. Bhatti, and Q. U. Islam, "Novel miniaturized Koch pentagonal fractal antenna for multiband wireless applications," *Progress In Electromagnetics Research*, Vol. 141, 693–710, 2013.
17. Aggarwal, A. and M. V. Kartikeyan, "Pythagoras tree: A fractal patch antenna for multi-frequency and ultra-wide bandwidth operations," *Progress Electromagnetics Research C*, Vol. 16, 25–35, 2010.
18. Mahmoud, A. M. M. K. R. and H. A. Elmikati, "Design of hexa-band planar inverted-F antenna using hybrid BSO-NM algorithm for mobile phone communications," *International Journal of RF and Microwave Computer-Aided Engineering*, Vol. 23, No. 1, 2013.
19. Lizzi, L., R. Azaro, G. Oliveri, and A. Massa, "Multiband fractal antenna for wireless communication systems for emergency management," *Journal of Electromagnetic Waves and Applications*, Vol. 26, No. 1, 1–11, 2012.
20. Balanis, C. A., *Antenna Theory: Analysis and Design*, 3rd Edition, Wiley, 2005.
21. Wu, Q., R. Jin, J. Geng, and M. Ding, "Pulse preserving capabilities of printed circular disk monopole antennas with different grounds for the specified input signal forms," *IEEE Trans. Antennas Propag.*, Vol. 55, No. 10, 2866–2873, Oct. 2007.